Thermodynamics of Ligand-Induced Assembly of Tubulin[†,‡]

José Fernando Díaz,[§] Margarita Menéndez,[∥] and José Manuel Andreu*[,§]

Centro de Investigaciones Biológicas, CSIC, Velázquez 144, and Instituto de Química-Física Rocasolano, CSIC, Serrano 118, 28006 Madrid, Spain

Received March 12, 1993; Revised Manuscript Received May 28, 1993

ABSTRACT: The equilibrium assembly of purified GDP–tubulin into microtubules induced by taxol and Taxotere has been studied as a function of solution variables, ligand, and nucleotide, in 10 mM sodium phosphate buffers. Assembly is coupled to the binding of one taxoid molecule per tubulin heterodimer, while binding to the unassembled protein is not detected within ligand solubility limits. Linked functions analysis has indicated that two Mg^{2+} and no more H^+ ions are bound per tubulin–taxoid polymerized, and the heat capacity change is negligible within experimental error (determined by van't Hoff analysis and by differential scanning calorimetry), in contrast with drug-free control microtubule assembly and with the abnormal polymerization of the tubulin–colchicine complex. The apparent enthalpy change is ca. 240 kJ mol^{-1} (calorimetry), and the process is entropy driven. The apparent standard free energy change of taxoid-induced elongation at 2 mM free Mg^{2+}, pH 6.1–6.7, and 37 °C is -29.5 ± 0.4 (taxol) or -31.5 ± 0.4 kJ mol^{-1} (Taxotere). This is independent of taxoid excess, which has indicated that the process measured corresponds to the elongation equilibrium of the fully liganded protein. Comparison to elongation in the absence of drug suggests an apparent linkage free energy change of binding and polymerization of -11.3 ± 1.2 kJ mol^{-1}. The taxoid-induced elongation of GTP–tubulin proceeds with an increment of apparent free energy change of -2.5 ± 0.4 kJ mol^{-1} over GDP–tubulin. It is proposed that the taxoid binding changes the conformation of GDP–tubulin from inactive to active, allowing productive binding and elongation at the microtubule end. Among several possible model mechanisms discussed, it is particularly attractive to think of taxoids as double-sided ligands, which bind to tubulin at the microtubule end and participate in a lateral contact interface with the newly added tubulin molecule. In the kinetic pathway of assembly, these ligands should bind first to inactive Mg^{2+}-induced linear GDP–tubulin oligomers and transform them into active bidimensional polymerization nuclei.

Microtubules are essential components of the cytoskeleton and constitute the target of antimitotic drugs. Microtubules are noncovalent helical polymers of the $\alpha\beta$ tubulin heterodimer, to which microtubule-associated proteins and cytoplasmic motors bind. The antitumor alkaloid taxol binds preferentially to microtubules more than to unassembled tubulin, and therefore induces assembly (Parness & Horwitz, 1981; Carlier & Pantaloni, 1983; Howard & Timasheff, 1988; Horwitz, 1992), by means of an unknown mechanism. The interaction of this ligand with unassembled tubulin has been regarded as much weaker than that with microtubules (Carlier & Pantaloni, 1983) or as practically undetectable (Takoudju et al., 1988; V. Peyrot and J. M. Andreu, unpublished).

The polymerization of highly purified tubulin induced by taxol constitutes a well-defined, simplified assembly model system, which has been employed to study the low-resolution structure of microtubules in solution (Andreu et al., 1991, 1992). It has recently been proven that taxol and the related drug Taxotere[1] induce the reversible assembly of purified GDP–tubulin, the inactive form of this protein, into microtubules, dispensing with the nucleotide γ-phosphate binding and hydrolysis, and that both ligands bind to exactly one site per tubulin dimer polymerized (Díaz & Andreu, 1993). The thermodynamic properties of this rigorous equilibrium system of ligand-induced microtubule assembly have now been examined. To gain a better understanding of how microtubule assembly is induced by these drugs, the effects of solution variables on taxol- and Taxotere-induced tubulin assembly in comparison to assembly without drugs, the thermal properties of drug-induced microtubules, and the linkage of polymerization to ligand binding have been studied. The results are reported in this paper, and model mechanisms of taxoid-induced tubulin assembly are examined.

MATERIALS AND METHODS

Preparation of GDP–tubulin, ligands, Mg^{2+} quantification, and microtubule assembly were as described (Díaz & Andreu, 1993). To facilitate rigorous comparison within the same experiments, GTP–tubulin was obtained by simple addition of GTP to aliquots of the same GDP–tubulin in presence of Mg^{2+} (Díaz & Andreu, 1993). Microtubule assembly experiments were done in PEDTA, 4 mM $MgCl_2$ buffer, pH 6.7, and 1 mM nucleotide(s) at 37 °C, employing equal total concentrations of taxoid and tubulin dimer, unless indicated otherwise. Measurement of taxoid binding to microtubules was performed by sedimentation at 50 000 rpm, 10–20 min,

† This work was supported in part by DGICyT Grant PB870220, Spanish–French joint actions (1990–1992), and a predoctoral fellowship from PNFPI to J.F.D.

‡ This paper is dedicated to Professor Serge N. Timasheff on the occasion of his 67th birthday.

§ Centro de Investigaciones Biológicas, CSIC.

∥ Instituto de Química-Física Rocasolano, CSIC.

[1] Abbreviations: GTP, guanosine triphosphate; GDP, guanosine diphosphate; Mes, 4-morpholineethanesulfonic acid; PEDTA, 10 mM phosphate, 1 mM ethylenediaminetetraacetic acid, pH as indicated; glyc-PEDTA, 3.4 M glycerol-containing PEDTA buffer; Taxol, 4,10-diacetoxy-2α-(benzoyloxy)-5β,20-epoxy-1,7β-dihydroxy-9-oxotax-11-en-13α-yl (2*R*,3*S*)-3-[(phenylcarbonyl)amino]-2-hydroxy-3-phenylpropionate; Taxotere (trademark of Rhône-Poulenc Rorer RP56976), 4-acetoxy-2α-(benzoyloxy)-5β,20-epoxy-1,7β,10β-trihydroxy-9-oxotax-11-en-13α-yl (2*R*,3*S*)-3-[(*tert*-butoxycarbonyl)amino]-2-hydroxy-3-phenylpropionate; HPLC, high performance liquid chromatography; DSC, differential scanning calorimetry.

0006-2960/93/0432-10067$04.00/0

in TLA100 and TLA100.2 rotors (Beckman) as described previously (Díaz & Andreu, 1993). It was verified that the pressure during centrifugation did not affect the polymerization, since the same critical concentration values were obtained by turbidity measurements, within experimental error.

Binding of Taxoids to Unassembled Tubulin. To measure the binding of ligands to unassembled tubulin by sedimentation (Medrano et al., 1991), taxol, Taxotere, or only dimethyl sulfoxide (usually 2.5%) were added to tubulin samples of known concentration in 1 mM GDP, 0 or 0.5 mM $MgCl_2$, and PEDTA buffer, pH 7.0 at 0–2 °C. The samples were incubated for 1 h at 37 °C and centrifuged for 1 h at 100 000 rpm in a prewarmed TLA 100 rotor in a TL-100 ultracentrifuge (Beckman), employing unused 200-μL polycarbonate tubes. At the end of the centrifugation the lower half of the tube contained the protein in equilibrium with the free ligand; the upper half contained only free ligand and essentially no protein, as checked by control measurements. The upper and lower 100 μL were carefully withdrawn, and the other drug was added as an internal standard (Taxotere for taxol measurements, and vice versa); 400 μL of methanol at −20 °C was added to precipitate the protein, the samples were centrifuged for 30 min in an Eppendorf microcentrifuge, and the supernatants were dried in a Savant SC-100 Speedvac. The taxoids were extracted from the dried samples by addition of 50 μL of methanol and analyzed in a reverse-phase column (Supelcosil LC-18-DB) in methanol:water (70:30, v/v) at a flow rate of 1 mL min^{-1} (Collins & Vallee, 1987). Alternately, [^{3}H]taxol or [^{14}C]Taxotere was employed instead of the unlabeled drugs, the samples were incubated and centrifuged as above, and the [^{3}H]taxol and [^{14}C]Taxotere concentrations in the upper and lower parts of the tube were measured by scintillation counting in an LKB 1219 spectrometer. In order to measure the binding of the taxoids to unassembled tubulin at the Mg^{2+} concentrations which induce assembly, the ligands were added to 28 μM tubulin samples in 1 mM GDP, 4 mM $MgCl_2$, and PEDTA buffer, pH 6.7, containing 5.6 μM podophyllotoxin (Aldrich), and the samples were essentially processed as above. The upper 90 μL contained free ligands and no protein, the lower 90 μL contained unassembled tubulin (ca. 15 μM) in equilibrium with free ligands, and the pellet contained assembled tubulin. Centrifugation of the tubulin–taxoid solution without the assembly inhibitor resulted in sedimentation of practically all the protein, which did not permit the measurement.

Differential Scanning Calorimetry. Heat capacity measurements were performed in a Microcal MC2 ultrasensitive differential scanning calorimeter, using the DA-2, Cpcalc, and Dynacp standard software packages for data collection and analysis. The calorimetric traces were recorded at a protein concentration of 50 μM and a scanning rate of 0.5 °C min^{-1}. Solutions were previously degassed, and a pressure of 2 atm was applied to avoid bubble formation in the calorimeter cell (Arriaga et al., 1992). In order to avoid thermal effects due to GTP hydrolysis (Hinz et al., 1979; Hinz & Timasheff, 1986), the calorimetric measurements of drug-induced assembly were performed with GDP–tubulin.

Thermodynamic Analysis of Assembly. The noncovalent nucleated condensation polymerization of protein assemblies is characterized by cooperative behavior and the presence of a critical concentration, C_r, below which no significant formation of the large polymer takes place. It can be easily shown that the apparent equilibrium constant for the growth reaction, i.e., the addition of a protomer to the polymer, is, in good approximation, equal to the reciprocal critical concentration,

$$K_p = C_r^{-1} \quad (1)$$

which renders the apparent standard free energy change of assembly amenable to simple measurement as a function of the solution variables. The analysis of the temperature dependence of K_p allows measurement of the van't Hoff enthalpy and heat capacity changes of the growth reaction (Oosawa & Asakura, 1975; Lee & Timasheff, 1977; Timasheff, 1981; Erickson & Pantaloni, 1981; Andreu et al., 1983; Erickson, 1989). The theory of linked functions (Wyman, 1964; Tanford, 1969; Aune et al., 1971; Lee & Timasheff, 1977; Timasheff, 1981; Wyman & Gill, 1990) can be employed to study the effect of any ligand in protein assembly. This theory predicts that when a ligand is involved in a conformational change or in a polymerization process, the equilibrium is displaced toward the species of greater binding. The preferential interaction of ligand X with protein P is defined as

$$\nu_X = (\delta m_X/\delta m_P)_{\mu_x, m_{i\neq p}} \quad (2)$$

where m_X and m_P are molal concentrations of ligand and protein. Under the assumption of a two-state reaction, it can be shown that the relationship between the ligand activity, a_x, and the polymer growth constant, K_p, at constant activity, a_i, of any other ligand is

$$[\delta(\ln K_p)/\delta(\ln a_x)]a_{i\neq x} = \Delta\nu_x \quad (3)$$

where $\Delta\nu_x$ is the difference in preferential binding of the ligand between the two end states of the reaction. If the ligand concentration is small enough to neglect the effects of the displacement of bound water, the measured value of $\delta(\ln K_p)/\delta(\ln a_x)$ becomes, in good approximation, the difference between the number of ligand molecules bound to the protein molecule in the polymer and monomer states (Lee & Timasheff, 1977).

Normal microtubule assembly is not a true equilibrium, due to the linked GTP hydrolysis and exchange, which generates dynamic instability. However, the drug-induced assembly of pure GDP–tubulin is clearly an equilibrium model reaction of microtubule polymerization. On the other hand, taxol-induced GTP–tubulin microtubules were shown to have diminished dynamic properties (Carlier & Pantaloni, 1983; Wilson et al., 1985) and behave similarly to GDP–tubulin microtubules (see Results), which indicates that the equilibrium analysis may be extended to them for the purposes of this study. Figure 1 shows representative results of drug-induced polymerization of GDP–tubulin and GTP–tubulin, which illustrate the cooperative behavior of the system. In these plots of assembled protein versus total protein concentration, the extrapolation to 0 of the amount of pelleted protein (microtubules) gives the critical concentration value, which is equal to the concentration of active protein in the supernatant. Since the slope of each plot is very near 1 (essentially all the added tubulin is active), the average tubulin concentration in the supernatant gives a very accurate measurement of critical concentration values.

RESULTS

Effects of Mg^{2+} and pH on Ligand-Induced Microtubule Polymerization. Since divalent cations are known to be required for tubulin assembly, the effect of Mg^{2+} activity on the taxol- and Taxotere-induced elongation of GTP–tubulin and GDP–tubulin was measured, and the results are shown

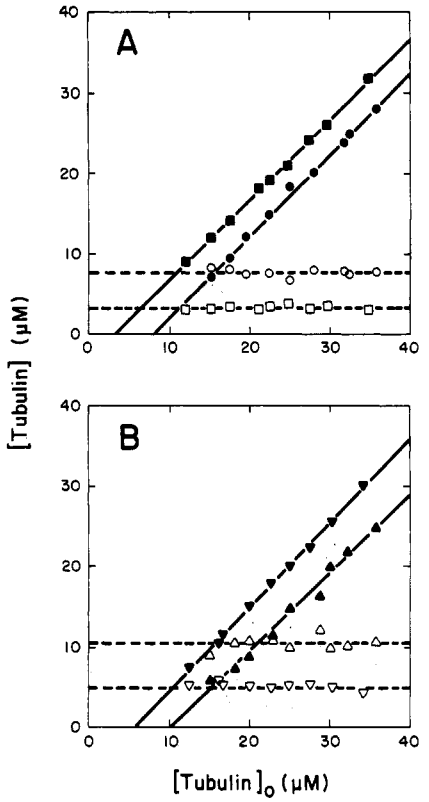

FIGURE 1: (A) Taxoid-induced polymerization of GTP–tubulin in PEDTA, 4 mM $MgCl_2$, 1 mM GDP, and 1 mM GTP, pH 6.7, 37 °C, measured by sedimentation: pelleted tubulin (Taxotere) (■), tubulin in supernatant (Taxotere) (□), pelleted tubulin (taxol) (●), and tubulin in supernatant (taxol) (○). (B) Taxoid-induced polymerization of GDP–tubulin under the same conditions without GTP: pelleted tubulin (Taxotere) (▼), tubulin in supernatant (Taxotere) (▽), pelleted tubulin (taxol) (▲), and tubulin in supernatant (taxol) (△).

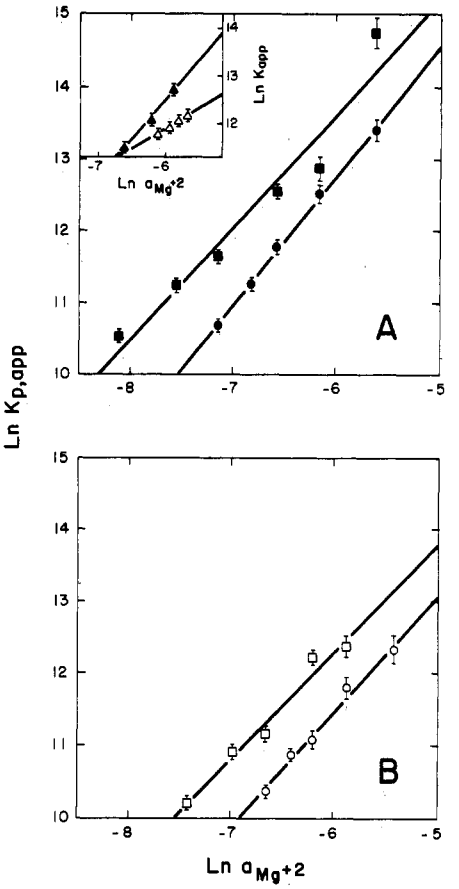

FIGURE 2: Wyman plots of taxol- and Taxotere-induced tubulin polymerization as a function of the activity of Mg^{2+} ions. The buffer was PEDTA and 1 mM GDP for GDP–tubulin (or 1 mM GDP plus 1 mM GTP for GTP–tubulin), pH 6.7, with $MgCl_2$ as variable at 37 °C. (A) GTP–tubulin: Taxotere ($MgCl_2$ concentrations are 2, 2.5, 3, 4, 5, and 7 mM) (■) and taxol ($MgCl_2$ concentrations are 3, 3.5, 4, 5, 7, mM) (●). The inset shows measurements in identical buffer plus 3.4 M glycerol (△) ($MgCl_2$ concentrations are 5.5, 6, 6.5, and 7 mM) or 3.4 M glycerol and taxol (▲) ($MgCl_2$ concentrations are 3, 4, and 5 mM). (B) GDP–tubulin: Taxotere ($MgCl_2$ concentrations are 2, 2.5, 3, 4, and 5 mM) (□) and taxol ($MgCl_2$ concentrations are 3, 3.5, 4, 5, and 7 mM) (○).

in Figure 2. The slopes of these Wyman linkage plots are between 1.46 and 1.78. These results essentially indicate a difference in preferential interaction, or binding, of two additional magnesium ions per tubulin molecule incorporated into the microtubule (see Materials and Methods). This is in contrast with the glycerol-induced assembly (Lee & Timasheff, 1977), in which only one more Mg^{2+} ion is bound per tubulin polymerized. Glycerol is a nonspecific thermodynamic enhancer of tubulin polymerization (Na & Timasheff, 1981). The inset in Figure 2A shows an increase of slope in the plot, from 0.89 to 1.66, which is induced by taxol in glycerol-containing buffer. This indicates that the additional cation bound can be attributed to the ligand binding and not to the cosolvent difference between both systems.

Magnesium was found to be absolutely required for taxoid-induced polymerization in phosphate buffer, in agreement with previous reports (Howard & Timasheff, 1988; Andreu et al., 1992). Equilibration of tubulin in 100 mM Mes and 0.1 mM GTP buffer, pH 6.5, allowed taxol-induced assembly with the residual ca. 75 μM Mg^{2+} (total) left in this preparation. Addition of 1 mM EDTA to the equilibration buffer (total Mg^{2+} left was ca. 35 μM) markedly weakened assembly, and further addition of 1 mM EDTA to the sample totally abolished polymerization, which later was completely recovered by the addition of 0.5 mM $MgCl_2$. Therefore in Mes buffer, which is known to interact with tubulin and to enhance microtubule assembly (Himes et al., 1977; Lee & Timasheff, 1977; Kay & Rosemeyer, 1986), much lower Mg^{2+} concentrations are effective, though the cation seems an absolute requirement for taxoid-induced assembly. Preliminary experiments have indicated a difference preferential interaction with Mg^{2+} per tubulin polymerized in Mes buffer significantly larger than 0. Taxol plus 300 μM Zn^{2+} induced the formation of sheets smaller than the characteristic Zn^{2+}-induced sheets (Gaskin & Kress, 1977). This low Zn^{2+} concentration was ineffective in PEDTA buffer, and large concentrations of this cation lead to the formation of amorphous tubulin precipitates.

The effect of hydrogen ions is shown in Figure 3A. The ligand-induced elongation is virtually pH independent in the ranges 6.1–6.9 for taxol and 6.1–6.7 for Taxotere (the slopes of the Wyman plots are –0.07 to 0.21), indicating that no additional proton is apparently bound or released from the protein in the polymerization. This is in agreement with the X-ray scattering measurements of taxol-induced assembly at pH 6.5–7.0 (Andreu et al., 1992) and in striking contrast with control glycerol-induced assembly, where one proton more is bound per tubulin polymerized (Lee & Timasheff, 1977). Figure 3B shows how taxol suppressed the pH dependence of assembly in glycerol buffer, confirming that the difference is due to the ligand binding and not to the absence of the cosolvent. An increase of C_r at higher pH was observed (more marked with Taxotere), which is partially reversible, since tubulin exposed to pH 7.3 during 5 min recovered its assembly capacity at pH 6.7. This agrees with the known sensitivity of

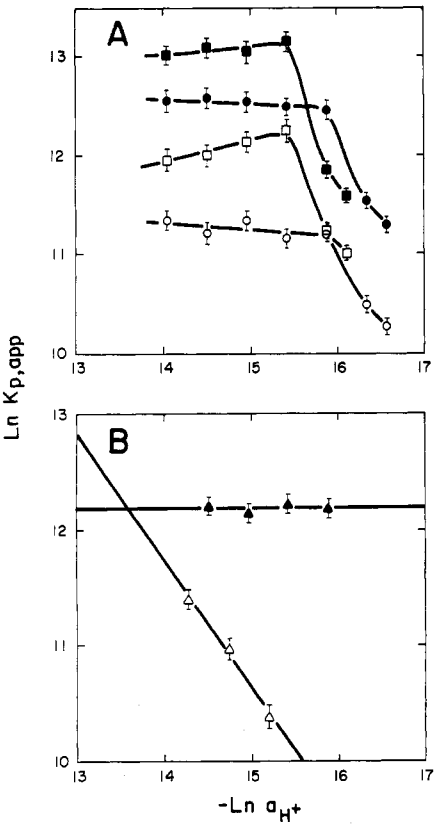

FIGURE 3: (A) Dependence of the apparent propagation constant of taxoid-induced polymerization on the hydrogen ion activity. The buffer was PEDTA, 4 mM $MgCl_2$, and 1 mM GDP (or 1 mM GDP plus 1 mM GTP), with the pH as variable, at 37 °C. Taxotere–GTP–tubulin (■), Taxotere–GDP–tubulin (□), taxol–GTP–tubulin (●), and taxol–GDP–tubulin (○). In these experiments the free Mg^{2+} concentration varied between 2.23 and 1.84 mM for the GDP measurements and between 1.55 and 1.31 mM for the GTP measurements, due to the variation of nucleotide affinity for the cation and the different phosphate buffer ionization. The values of ln K_{app} were corrected to a free Mg^{2+} concentration of 2.01 mM prior to plotting. (B) Wyman plots of tubulin polymerization in PEDTA buffer containing 3 mM $MgCl_2$, 1 mM GDP, 1 mM GTP, and 3.4 M glycerol, at 37 °C, with (▲) or without taxol (△), as a function of the activity of H^+ ions. The taxol data were corrected to 1.27 mM free Mg^{2+}. The values of $-\ln a_{H^+}$ can be converted into pH by dividing by 2.303.

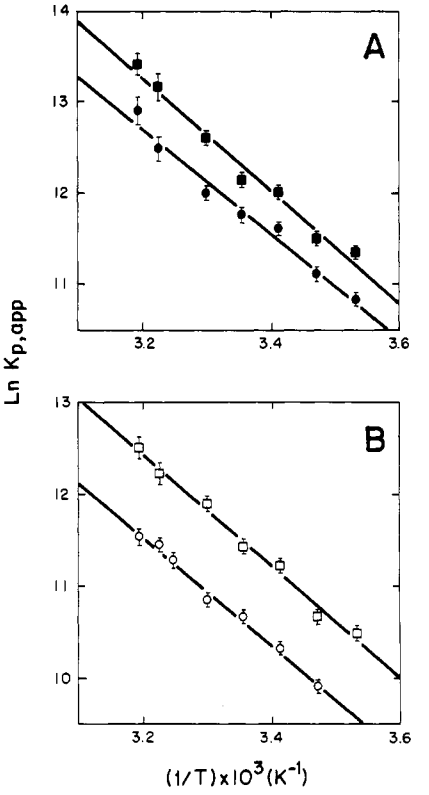

FIGURE 4: Van't Hoff plot of taxoid-induced microtubule elongation. (A) GTP–tubulin in PEDTA, 4 mM $MgCl_2$, 1 mM GDP, and 1 mM GTP, pH 6.7 (data corrected to 2.01 mM free Mg^{2+}): Taxotere (■) and taxol (●). (B) GDP–tubulin in PEDTA, 4 mM $MgCl_2$, and 1 mM GDP, pH 6.7: Taxotere (□) and taxol (○).

microtubule assembly to alkaline pH (Gaskin et al., 1974; Ringel & Horwitz, 1991). At pH values below 6.1, tubulin started to precipitate, interfering with the measurement of assembly.

Temperature Dependence and Differential Scanning Calorimetry of Ligand-Induced Tubulin Assembly. The temperature dependence of the drug-induced elongation of GTP–tubulin and GDP–tubulin is shown in panels A and B, respectively, of Figure 4. The van't Hoff plots of drug-induced elongation are virtually linear, with negligible $\Delta C^\circ_{p,app}$, and ΔH°_{app} values near 50 kJ mol^{-1} in all cases (Table I). This is again different from the thermodynamic parameters of the drugless assembly in glycerol buffer, which proceeds with a significant heat capacity change (Lee & Timasheff, 1977).

Microtubule assembly induced by taxol or Taxotere was also examined by differential scanning calorimetry under the same buffer conditions. The results are shown in Figure 5 and Table II. The drug-induced polymerization of tubulin was endothermic and proceeded with nil heat capacity change, within experimental error (see trace a in Figure 5). This coincides qualitatively with the results derived from the van't Hoff analysis. To verify that the transition seen in the heat capacity function was actually due to the tubulin polymerization process, turbidity experiments were performed in which an aliquot of the same tubulin solution employed in calorimetry was heated at 0.5 °C min^{-1}. The increase of turbidity took place in the temperature range of the calorimetric transition, although the midpoint was somewhat shifted toward high temperature. Control experiments without the drug added to the GDP–tubulin solution (trace b of Figure 5) showed that the transition requires the presence of taxol or Taxotere. The assembly of GDP–tubulin with taxol in glycerol-containing buffer also proceeded without significant heat capacity change (trace c); this is distinct from GTP–tubulin polymerization in glycerol-containing buffer (trace d), for which the increase in heat capacity was found to be -6700 ± 600 J mol^{-1} K^{-1}, which is compatible with the results reported by Hinz et al. (1979) and Hinz and Timasheff (1986). The disappearance of the heat capacity change is due to the ligand, not to the absence of the cosolvent. Under nonassembly conditions (low Mg^{2+} concentrations) no transition was detected in the temperature range at which the assembly of tubulin was normally observed (trace e of Figure 5), and the denaturation profiles of tubulin in the presence of 1 mol of ligand per tubulin dimer were in agreement with those obtained in the absence of the ligand (Table II). These calorimetric results show the requirement for Mg^{2+} of the drug-induced polymerization of tubulin and also suggest that the binding of taxol and Taxotere to unassembled tubulin would probably be very weak or nonexistent. A more detailed examination of the system at varying Mg^{2+} concentration showed the complexity of processes involved in taxoid-induced polymerization of tubulin. The shape of the calorimetric transition and the enthalpy of assembly were dependent on the cation concentration (traces a, f, and g of Figure 5) and the ligand employed (traces h and a). At the lower Mg^{2+} concentrations the heat uptake pattern

Table I: Properties of the Taxoid-Induced Microtubule Elongation Equilibrium in Comparison with Glycerol-Induced Elongation

property	taxol	Taxotere	3.4 M glycerol
$\Delta\nu_{H^+}$	-0.07 ± 0.05^a	-0.06 ± 0.05^a	
	0.21 ± 0.07^b	0.08 ± 0.05^b	$1.00 \pm 0.22,^b$ 0.86^c
$\Delta\nu_{Mg^{2+}}$	1.58 ± 0.03^a	1.46 ± 0.10^a	
	1.78 ± 0.03^b	1.55 ± 0.03^b	$0.89 \pm 0.05,^b$ 0.78^c
$\Delta G°_{app}$ (kJ mol^{-1}, 37 °C)^d	-29.51 ± 0.40^a	-31.49 ± 0.45^a	
	-32.16 ± 0.38^b	-33.88 ± 0.35^b	$-28.01 \pm 0.5,^f$ $-27.13^{c,e}$
$\Delta H°_{app}$ (kJ mol^{-1})^{d,g}	49.10 ± 0.05^a	50.42 ± 0.05^a	
	47.62 ± 0.05^b	51.63 ± 0.05^b	8.96^c (37 °C)
$\Delta S°_{app}$ (J mol^{-1} K^{-1})^{d,g}	253 ± 4^a	264 ± 5^a	
	257 ± 3^b	276 ± 3^b	116^c (37 °C)
$\Delta C°_{p,app}$ (J mol^{-1} K^{-1})^{d,g}	0 ± 300^a	0 ± 300^a	
	0 ± 300^b	0 ± 300^b	-6250 ± 1250^c

[a] GDP–tubulin. [b] GTP–tubulin. [c] GTP–tubulin data from Lee and Timasheff (1977). [d] Data obtained at 2.01 mM free Mg^{2+}, pH 6.7. [e] Data corrected to 2.01 mM free Mg^{2+}, pH 6.7 (original data at 11.75 mM free Mg^{2+}, pH 7.0). [f] Data corrected to 2.01 mM free Mg^{2+}, pH 6.7 (original data at 3.21 mM free Mg^{2+}, pH 6.5). [g] From van't Hoff analysis.

Table II: Enthalpy and Heat Capacity Changes of Tubulin Assembly and of Thermal Denaturation of Microtubules Determined by Differential Scanning Calorimetry

		assembly[a]		denaturation	
ligand and protein	buffer (pH 6.7)	ΔH (kJ mol^{-1})	ΔC_p (J mol^{-1} K^{-1})	T_m (°C)	ΔH (kJ mol^{-1})
GDP–tubulin	PEDTA, GDP, 0.5 mM Mg^{2+}			54.8	724 ± 30
GDP–tubulin	PEDTA, GDP, 1.5 mM Mg^{2+}			55.6	777 ± 54
GDP–tubulin	PEDTA, GDP, 4 mM Mg^{2+}			56.2	849 ± 60
Taxotere, GDP–tubulin	PEDTA, GDP, 2 mM Mg^{2+}			55.1	765 ± 53
Taxotere, GDP–tubulin	PEDTA, GDP, 3 mM Mg^{2+}	221 ± 10	0 ± 500	59.5, 63.3[b]	950 ± 66
Taxotere, GDP–tubulin	PEDTA, GDP, 3.5 mM Mg^{2+}	240 ± 9	0 ± 500	59.5, 64.4[b]	1000 ± 80
Taxotere, GDP–tubulin	PEDTA, GDP, 4 mM Mg^{2+}	104 ± 10	0 ± 500	66.0	1309 ± 75
taxol, GDP–tubulin	PEDTA, GDP, 0.5 mM Mg^{2+}			54.0	828 ± 58
taxol, GDP–tubulin	PEDTA, GDP, 4 mM Mg^{2+}	214 ± 8	0 ± 500	64.4	1305 ± 95
taxol, GDP–tubulin	glyc-PEDTA, GDP, 3 mM Mg^{2+}	96 ± 10	0 ± 500	62.8	1440 ± 97
taxol, GDP–tubulin	glyc-PEDTA, GDP, 4 mM Mg^{2+}	n.d.	n.d.	65.5	1441 ± 95
GDP–tubulin	glyc-PEDTA, GDP, 6 mM Mg^{2+}			60.1	1146 ± 80
GTP–tubulin	glyc-PEDTA, GTP, 6 mM Mg^{2+}	87 ± 14	-6700 ± 600	61.3	1096 ± 66

[a] Values are given per mole of assembled protein. [b] These DSC denaturation profiles were bimodal, possibly due to a significant fraction of unassembled protein.

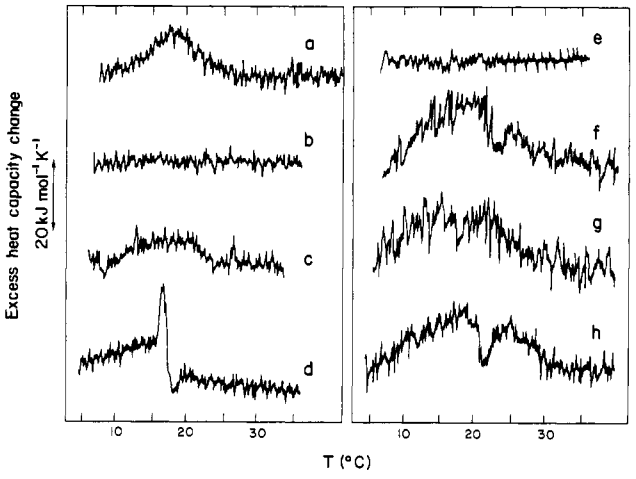

FIGURE 5: Scans of the apparent heat capacity change of 50 μM tubulin in PEDTA buffer, pH 6.7, under varying assembly conditions; scan rate, 0.5 °C/min. Trace a, 1 mM GDP, 4 mM $MgCl_2$, and Taxotere; trace b, 1 mM GDP and 4 mM $MgCl_2$; trace c, 1 mM GDP, 3.4 M glycerol, 3 mM $MgCl_2$, and taxol; trace d, 1 mM GTP, 3.4 M glycerol, and 6 mM $MgCl_2$; trace e, 1 mM GDP, 2 mM $MgCl_2$, and Taxotere; trace f, 1 mM GDP, Taxotere, and 3 mM $MgCl_2$; trace g, same as trace f but 3.5 mM $MgCl_2$; trace h, 1 mM GDP, 4 mM $MgCl_2$, and taxol.

is complex, being characterized by an inflection point whose position depends on both the drug and the Mg^{2+} concentration used. Increasing cation concentrations displace the transition to lower temperatures and modify the heat capacity traces, so that the inflection point is not observed with Taxotere at 4 mM Mg^{2+} and the apparent enthalpy change decreases toward the value derived from the van't Hoff plots. The slowness of the microtubule assembly process, particularly at a low temperature, makes the temperature increase in DSC too rapid for the reaction to reach equilibrium, which would only be attained at the initial and final states of the transition. Therefore, the heat uptake profile should be a function of temperature and the kinetic rate constants of the reaction, and the gradual increase in temperature could help to resolve slow reactions. Then the modifications observed in the DSC profiles of Taxotere-induced assembly at varying Mg^{2+} concentrations would probably be a consequence of the effects of the cation on the tubulin polymerization kinetics. The enthalpy of taxol-induced assembly at 4 mM Mg^{2+} compares with the enthalpy of Taxotere-induced assembly below 4 mM Mg^{2+} (Table II). The disappearance of the inflection point with the concomitant decrease of the apparent assembly enthalpy and the shape change of the experimental heat capacity profile at high Mg^{2+} concentrations or in buffer with glycerol suggest the occurrence of early events which, under these experimental conditions, could be fast enough to have already taken place below 6–7 °C. Less likely, the inflection would be caused by an uncharacterized exothermic transition in the system superimposed on a broad endotherm, as occasionally observed by Hinz and Timasheff (1986), who employed tubulin with a nonhydrolyzable GTP analogue.

Thermal Stability of Microtubules. Figure 6 shows the DSC profiles of the irreversible thermal denaturation of unassembled and assembled tubulin under several conditions. Thermal denaturation of tubulin is a kinetically controlled process (not shown), giving skewed DSC profiles (Sanchez-

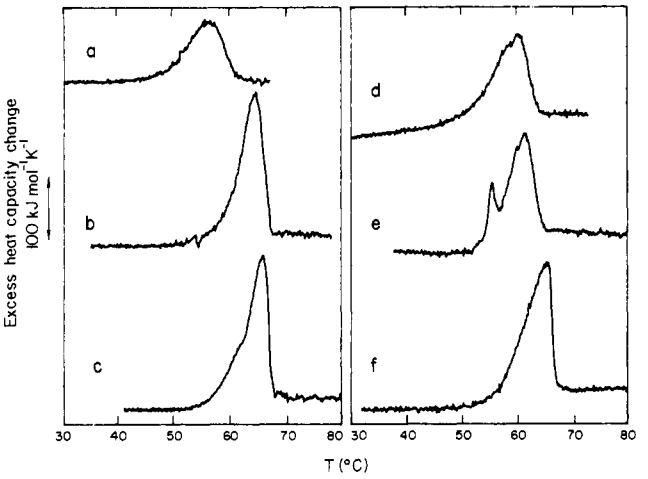

FIGURE 6: DSC profiles of thermal denaturation of polymerized and unassembled tubulin (50 μM) in PEDTA buffer, pH 6.7, under different solvent conditions; scan rate, 0.5 °C/min. Trace a, 1 mM GDP and 4 mM $MgCl_2$; trace b, 1 mM GDP, 4 mM $MgCl_2$, and taxol; trace c, 1 mM GDP, 4 mM $MgCl_2$, and Taxotere; trace d, 1 mM GDP, 6 mM $MgCl_2$, and 3.4 M glycerol; trace e, 1 mM GTP, 6 mM $MgCl_2$, and 3.4 M glycerol; trace f, 1 mM GDP, 4 mM $MgCl_2$, 3.4 M glycerol, and taxol.

Ruiz et al., 1988), and for this reason comparison of thermal denaturation parameters for unassembled and polymerized tubulin has been done in terms of the T_m and ΔH_d values obtained at the same scanning rate, which are summarized in Table II. The assembly of GDP–tubulin with taxol or Taxotere stabilizes the protein against thermal denaturation (traces a, b, and c) and increases the asymmetry of the transition, as expected for an aggregating system (Wyman & Gill, 1990). The T_m value is shifted toward higher temperatures by about 10 °C, and the denaturation enthalpy is increased by 460 kJ mol^{-1} in PEDTA buffer at 4 mM Mg^{2+}. The T_m and denaturation enthalpy values of polymerized tubulin increase with Mg^{2+} concentration. Thermal denaturation of microtubules resulted in extensive protein aggregation, which is not observed in unassembled tubulin (Mozo-Villarías et al., 1991). As expected, GDP–tubulin in GAB buffer does not assemble, and its thermal denaturation proceeds with a maximum in heat capacity at 60.1 °C and an enthalpy change of 1146 kJ mol^{-1} (Figure 6, trace d). These values are only slightly modified by assembly of tubulin in glycerol buffer with GTP (trace e). The denaturation profile of GDP–tubulin assembled with taxol in glycerol buffer with 4 mM Mg^{2+} (trace f) is similar to that obtained without glycerol (trace b). Since thermal denaturation of tubulin is independent of having GTP or GDP at the exchangeable site (unpublished data), these results indicate that a significant part of the thermal stabilization of taxoid-induced microtubules was conferred by the binding of the taxoid to microtubules rather than by tubulin assembly itself. The experimental ΔC_p of denaturation of microtubules was found to decrease with Mg^{2+} concentration and to increase with glycerol. Its value varied from 44 ± 4 kJ mol^{-1} K^{-1}, in the presence of glycerol or at 3 mM Mg^{2+}, to 20 ± 2 kJ mol^{-1} K^{-1} at 4 mM Mg^{2+} in absence of cosolvent.

Linkage of Ligand Binding to Microtubule Polymerization. Lack of Detectable Binding of Taxol and Taxotere to Unassembled Tubulin. Since taxol induces microtubule assembly by preferential binding to the polymer, the possible interactions of taxol and Taxotere with the tubulin dimer were critically examined first. Purified calf brain tubulin without added Mg^{2+} has a sedimentation velocity coefficient (Frigon & Timasheff, 1975a) and an X-ray scattering radius of gyration (Andreu et al., 1989) corresponding to the monodisperse $\alpha\beta$ heterodimer, even at high protein concentrations. High-speed sedimentation of 15–20 μM tubulin solutions containing up to 50 μM Taxotere or 10 μM taxol in buffer containing 0 or 0.5 mM Mg^{2+}, followed by HPLC and radioactive ligand measurements, permitted us to ascertain negligible binding of both ligands, which indicates equilibrium constants of binding to the unassembled dimer smaller than 10^3 M^{-1}, as shown by Figure 7C. Next, in a different experiment in Mg^{2+}-containing buffer, the ligand binding and the polymerization of GTP–tubulin were simultaneously quantified by low-speed sedimentation, as a function of Taxotere and taxol concentration. The results are shown in panels A and B, respectively, of Figure 7. The ordinates of these figures are sedimented ligand and sedimented protein, both divided by total protein concentration. The abscissa axes

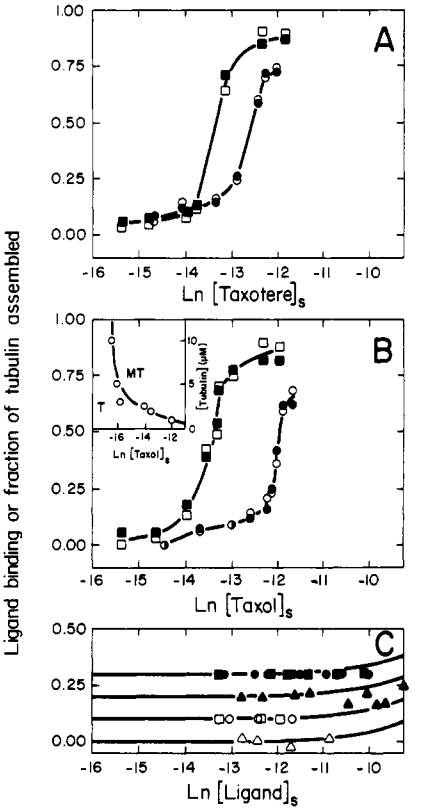

FIGURE 7: (A) Binding of Taxotere to tubulin in PEDTA, 1 mM GDP, 1 mM GTP, and 8 mM $MgCl_2$ buffer, pH 6.7, 37 °C, measured by sedimentation, employing [^{14}C]Taxotere. Binding is expressed in moles of ligand per 10^5 g of tubulin: ligand bound to 1.5 μM total tubulin (□), fraction of tubulin assembled in the same experiment (■), Taxotere bound to 0.9 μM total tubulin (○), and fraction of tubulin assembled in the same experiment (●). The lines are drawn solely to show the trend of the data. (B) Binding of taxol to tubulin under the same conditions, measured by sedimentation and HPLC quantification of taxol: ligand bound to 2.5 μM total tubulin (□), fraction of tubulin assembled in the same experiment (■), ligand bound to 1.0 μM total tubulin (○), and fraction of tubulin assembled (●). The inset shows an approximate phase diagram of tubulin assembly into microtubules under the same conditions; the protein is unassembled (T) below the line, and microtubules (MT) are observed above the line. (C) Taxoid binding to unassembled tubulin in PEDTA, 1 mM GDP, and 0–4 mM $MgCl_2$, pH 6.7, 37 °C, measured by employing [^{14}C]Taxotere and [^{3}H]taxol: binding of Taxotere to 20 μM tubulin without $MgCl_2$ (points are displaced by 0.3 in the y-axis to facilitate comparison) (●) or with 0.5 mM $MgCl_2$ (■); binding of Taxotere to 15 μM tubulin with 4 mM $MgCl_2$ and 5.6 μM podophyllotoxin (points are displaced 0.2 in the y-axis) (▲); binding of taxol to 20 μM tubulin without $MgCl_2$ (points are displaced by 0.1 in the y-axis) (○) or with 0.5 mM $MgCl_2$ (□); and binding of taxol to 15 μM tubulin with 4 mM $MgCl_2$ and 5.6 μM podophyllotoxin (△). The solid lines are theoretical binding isotherms with a binding equilibrium constant of 10^3 M^{-1}.

are ligand concentration in the supernatant. Neglecting the very small volume of the pellet and ligand binding to the protein left in the supernatant,[2] the results of the experiment are, in good approximation, the number of molecules of ligand bound per tubulin dimer and the fraction of protein polymerized, both as functions of ligand activity. The two processes, binding and assembly, are coincident, and there is no unliganded tubulin assembled, or liganded protein unassembled, within experimental error. The binding and polymerization isotherms are very cooperative, reminiscent of a phase change. The inset of Figure 7B is an approximate phase diagram of the tubulin–taxol system, which indicates the protein and ligand concentrations above which assembly is observed. Finally, the taxoid-induced assembly in 4 mM Mg^{2+}-containing buffer was partially inhibited by a substoichiometric concentration of podophyllotoxin, and after high-speed sedimentation the binding of taxoids to unassembled tubulin (dimer and oligomers) was negligible (Figure 7C).

DISCUSSION

Apparent Thermodynamic Parameters of Taxol- and Taxotere-Induced Microtubule Assembly. Comparison to Other Tubulin Assembly Reactions. Table I summarizes the properties of the taxol- and Taxotere-induced microtubule polymerization in comparison to assembly without drug in glycerol-containing buffer. The ligand-induced differences in the preferential interactions with H^+ and Mg^{2+} and in the heat capacity and enthalpy changes are striking: the assembly process is thermodynamically different, yet in both systems the end structures are microtubules. Taxoid binding stabilizes microtubules against thermal denaturation. On the other hand, the polymerization of the tubulin–colchicine complex into abnormal non-microtubule polymers was shown to be characterized by thermodynamic parameters very close to those of microtubule assembly (Andreu et al., 1983). The apparent enthalpy and entropy contributions to the free energy change of the growth reaction of taxoid- and glycerol-induced assembly and the tubulin–colchicine abnormal polymerization are shown in panels A, B, and C, respectively, of Figure 8. The nil total heat capacity change and the moderate enthalpy change of the taxol- and Taxotere-induced assembly allow observation of the reaction even in the cold (Andreu et al., 1992), whereas the critical concentration of normal microtubule assembly increases markedly at low temperature, hampering observation (Lee & Timasheff, 1977). The polymerization of tubulin–colchicine in the presence of taxol proceeds with heat capacity and enthalpy changes (Howard & Timasheff, 1988) similar to the taxol-induced microtubule assembly. While taxol and Taxotere induce essentially normal microtubule polymers with thermodynamics markedly different from the assembly without drug, bound colchicine induces abnormal polymers with "normal" thermodynamics. This paradox is only apparent because the binding of the ligand is not included in the later measurement, and bound colchicine may induce minor changes in the nature of the contacts between tubulin molecules but only a small geometric distortion leading to the abnormal polymer (Andreu et al., 1983), while in the taxoid-induced microtubule assembly the linked processes of polymerization and ligand binding are measured.

[2] The pellet volume was smaller than 2.5% of the total volume. Control experiments at greater protein concentration in excess over ligand concentration showed that essentially all ligand was sedimented; i.e., none was bound to the protein in the supernatant.

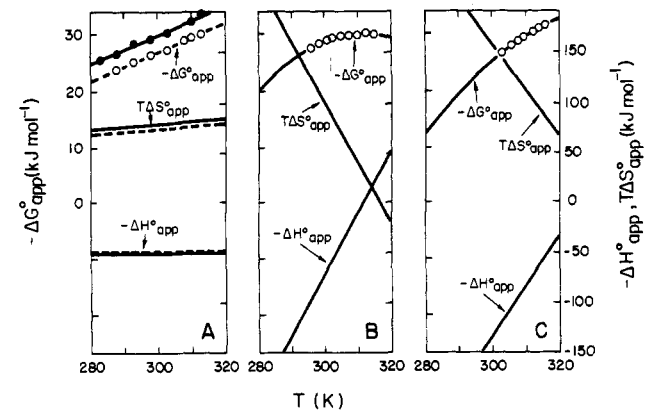

FIGURE 8: (A) Enthalpy and entropy contributions to the apparent standard free energy change of elongation of GDP–tubulin in 1 mM GDP, 2.01 mM free Mg^{2+}, and PEDTA buffer, pH 6.7, induced by Taxotere (—, ●) and taxol (—, ○). (B) Enthalpy and entropy contributions to the apparent standard free energy change of elongation of tubulin in 1 mM GTP, 3.4 M glycerol, 1 mM EGTA, 11.75 mM free Mg^{2+}, and 10 mM phosphate buffer pH 7.0 (Lee & Timasheff, 1977). The glycerol-induced assembly data in this plot were obtained at larger free Mg^{2+} concentration than the taxol data; therefore, their absolute free energy change values are shifted. However, the heat capacity change of the glycerol assembly system is similar, at Mg^{2+} concentrations and pH values identical to those of the taxol assembly (Table II), which validates the comparison of the temperature dependence of the thermodynamic parameters in the figure. (C) Enthalpy and entropy contributions to the apparent standard free energy change of polymerization of tubulin–colchicine complex in 1 mM GTP, 12.85 mM free Mg^{2+}, and 10 mM phosphate buffer, pH 7.0 (Andreu et al., 1983).

Scheme I

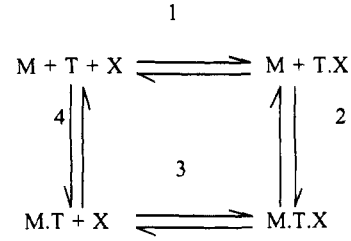

Scheme II

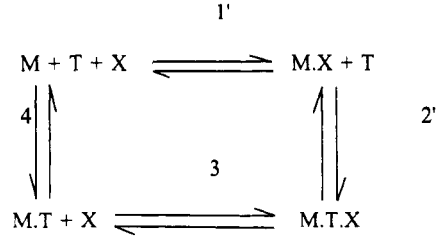

Linkage of Ligand Binding to Microtubule Polymerization. Taxol and Taxotere have not been observed to bind appreciably to the tubulin dimer but do bind with high apparent affinity to microtubules. The simplest hypothesis is that the binding site for taxoids should be at some portion of the tubulin–tubulin contact area and/or be due to the conformation characteristic of the assembled protein. The ligand-induced elongation of microtubules can be formally described by the set of linked equilibria in Scheme I (Lee & Timasheff, 1977), where M, T, and X are the microtubule end, tubulin, and taxoid ligands, respectively. Reactions 1 and 2 constitute the ligand-mediated pathway (binding precedes elongation), while reactions 4 and 3 are the ligand-facilitated pathway (elongation precedes binding). It can also be conceived that the ligand binds to the microtubule end, as in Scheme II. The standard

free energy change of the overall binding and association process is (Scheme I)

$$\Delta G^\circ_{over} = \Delta G^\circ_1 + \Delta G^\circ_2 = \Delta G^\circ_3 + \Delta G^\circ_4 \quad (4)$$

The apparent linkage free energy coupling the binding of ligand to the protein association is (Cantor & Schimmel, 1980, p 874)

$$\Delta G^\circ_{linkage} = \Delta G^\circ_2 - \Delta G^\circ_4 = \Delta G^\circ_3 - \Delta G^\circ_1 = \Delta G^\circ_{over} - \Delta G^\circ_1 - \Delta G^\circ_4 \quad (5)$$

which has to be significantly negative (i.e., $K_3 \gg K_1$, $K_2 \gg K_4$) for the ligand to induce elongation and includes any other linked processes implicit in the individual equilibria. Given the fact that the sedimentation method employed to measure polymerization does not distinguish liganded from unliganded protein, the apparent equilibrium growth constant which is actually measured is (Scheme I)

$$C_r^{-1} = K_{p,app} = ([M\cdot T] + [M\cdot T\cdot X])/([M]([T] + [TX])) \quad (6)$$

$$K_{p,app} = K_1K_2([X] + 1/K_3)/(1 + K_1[X]) \quad (7)$$

Therefore the apparent standard free energy change measured is

$$\Delta G^\circ_{app} = -RT \ln K_{p,app} = \Delta G^\circ_1 + \Delta G^\circ_2 + RT \ln (1 + K_1[X]) - RT \ln ([X] + 1/K_3) \quad (8)$$

which is different from the true overall free energy change, ΔG°_{over} (eq 4) because of the last two terms. The van't Hoff standard enthalpy and heat capacity changes are

$$\Delta H^\circ_{app} = -R\, d(\ln K_{app})/d(1/T)$$
$$= \Delta H^\circ_1 + \Delta H^\circ_2 + R\, d[\ln(1 + K_1[X])]/d(1/T) - R\, d[\ln([X] + 1/K_3)]/d(1/T)$$
$$= \Delta H^\circ_2 + \Delta H^\circ_1/(1 + K_1[X]) - \Delta H^\circ_3/(1 + K_3[X]) \quad (9)$$

$$\Delta C^\circ_{p,app} = d(\Delta H^\circ_{app})/dT$$
$$= \Delta C_{p1} + \Delta C_{p2} + R\, d^2[\ln(1 + K_1[X])]/d(1/T)\, dT - R\, d^2[\ln([X] + 1/K_3)]/d(1/T)\, dT$$
$$= \Delta C_{p2} + \Delta C_{p1}/(1 + K_1[X]) - \Delta H_1^2K_1[X]/RT^2(1 + K_1[X])^2 - \Delta C_{p3}/(1 + K_3[X]) + \Delta H_3^2K_3[X]/RT^2(1 + K_3[X])^2 \quad (10)$$

The apparent difference in preferential ligand binding (eq 3) is

$$\Delta \nu_{x,app} = \Delta \nu_{x1} + \Delta \nu_{x2} - \delta[\ln(1 + K_1[X])]/\delta(\ln a_x) + \delta[\ln([X] + 1/K_3)]/\delta(\ln a_x) = \Delta \nu_{x2} + (\Delta \nu_{x1} - K_1[X])/(1 + K_1[X]) - (\Delta \nu_{x3} - K_3[X])/(1 + K_3[X]) \quad (11)$$

Equations 7–11 with the appropriate substitutions apply equally to Scheme II. If only the ligand-mediated pathway of the schemes operates, eq 8 is modified to

$$\Delta G^\circ_{app} = \Delta G^\circ_1 + \Delta G^\circ_2 + RT \ln(1 + K_1[X]) - RT \ln[X] \quad (12)$$

which at $[X] \gg K_1^{-1}$ becomes independent of [X], as eq 8 does. If only the ligand-facilitated pathway of the schemes operates, eq 8 is modified to

$$\Delta G^\circ_{app} = \Delta G^\circ_3 + \Delta G^\circ_4 - RT \ln([X] + 1/K_3) \quad (13)$$

which at $[X] \gg K_3^{-1}$ diminishes indefinitely with growing [X]. A crucial experimental observation in our system is that the values of $\Delta G^\circ_{app} = RT \ln C_r$ were independent of excess ligand concentration, under all the conditions employed to measure C_r in the study [Figures 1–4; Figure 5 in Díaz and Andreu (1993)]. Such an observation indicates the participation of the ligand-mediated pathway. This does not exclude the simultaneous operation of the ligand-facilitated pathway of protein association and does not indicate a preferred pathway, as also discussed by Na and Timasheff (1980). What is more important, in order to obtain these saturation conditions, it must hold that $[X] \gg K_1^{-1} > K_3^{-1}$, and therefore eqs 8–11 simplify in good approximation to

$$\Delta G^\circ_{app} \approx \Delta G^\circ_2 \quad (14)$$

$$\Delta H^\circ_{app} \approx \Delta H^\circ_2 \quad (15)$$

$$\Delta C_{p,app} \approx \Delta C_{p2} \quad (16)$$

$$\Delta \nu_{x,app} \approx \Delta \nu_{x2} \quad (17)$$

Therefore, what we have actually measured is the elongation of the taxoid-liganded protein, be it unassembled (Scheme I) or in microtubules (Scheme II). Its free energy, enthalpy, and heat capacity changes are also apparent parameters which are influenced by the linkage to the binding of any other ligand $Y \neq X$ in the system, such as the Mg^{2+} ion. At intermediate ligand concentrations (see Figure 7), if conditions were met in which $K_1^{-1} \gg [X] \gg K_3^{-1}$, eqs 8 and 12 would simplify to

$$\Delta G^\circ_{app} \approx \Delta G^\circ_1 + \Delta G^\circ_2 - RT \ln[X] \quad (18)$$

and under said conditions the apparent free energy change would decrease linearly with increasing ln[X], the same as in a Wyman plot of unitary slope (eq 3, Materials and Methods). Finally, at very low ligand concentrations, or in the absence of the ligand, i.e., $K_1^{-1} > K_3^{-1} \gg [X]$, what would be measured is the elongation of the unliganded protein:

$$\Delta G^\circ_{app} \approx \Delta G^\circ_4 \quad (19)$$

The value of the observed free energy change for the taxol-induced assembly of GTP–tubulin in phosphate buffer, pH 6.7, at 2 mM free Mg^{2+} and 37 °C was -32.2 ± 0.4 kJ mol^{-1} (Table I; -33.9 ± 0.4 kJ mol^{-1} for Taxotere). The taxol-independent assembly, reaction 4 in Schemes I and II, would only be possible at very high protein concentrations under our conditions. Its standard free energy change, ΔG°_4, can be approximately estimated as -21.7 ± 1.7 kJ mol^{-1}, from the data in glycerol (Table I), after correction for the glycerol absence employing the approximation described by Lee and Timasheff (1977). Therefore, by application of eq 5 the linkage free energy of the system can be estimated to be -10.5 ± 1.2 kJ mol^{-1} (-12.2 ± 1.2 kJ mol^{-1} for Taxotere). This is close to an independent estimation of the linkage free energy provided by taxol binding (Howard & Timasheff, 1988) of ca. -12.5 kJ mol^{-1}. A totally rigorous estimation is precluded due to the required comparison of drugless assembly with the linked GTP hydrolysis, which is not a strictly equilibrium condensation polymerization system.[3] The conclusion that equilibrium 1 or 1′ is essentially (i.e., more than 90%) displaced to the bound species at the free ligand concentrations employed to induce maximal assembly (around 4×10^{-6} M) implies that $\Delta G^\circ_{1or1'} \leq -38$ kJ mol^{-1}, and therefore (eqs 4 and 5) $\Delta G^\circ_{over} \leq -70$ kJ mol^{-1} and $\Delta G^\circ_3 \leq -48$ kJ mol^{-1}, and suggests that the binding of taxol to microtubules is a strong interaction. Its equilibrium binding constant would be $K_3 \geq 10^8$ M^{-1} under

our conditions if reaction 3 could be isolated. Scheme I together with eq 14 implies practical saturation of binding equilibrium 1 under the assembly conditions. This is in marked contrast with the lack of detectable binding of taxol and Taxotere to tubulin at low Mg^{2+} concentrations or with podophyllotoxin (Figure 7C), although reaction 1 could not be isolated and measured under conditions identical to the assembly experiment. On the other hand, Scheme II with eq 14 is not in contradiction with other measurements, since the affinity of reaction 1′ is unknown.

On the basis that the reaction which is being measured is the apparent equilibrium association of the taxoid-liganded protein (reaction 2 or 2′), if the contribution of glycerol to the enthalpy of elongation could be neglected in a first approximation (Table II and discussion above), the above comparison to the association without ligand (reaction 4) might be extended to the rest of the thermodynamic parameters determined (eqs 9–11). Thus, the values of the linkage apparent standard enthalpy and entropy changes, defined similarly to eq 5, would respectively be ca. 40 kJ mol^{-1} and about 150 J mol^{-1} K^{-1} at 37 °C (from the van't Hoff analysis), and the value of the linkage apparent heat capacity change would be ca. 6 kJ mol^{-1} K^{-1}. These values include contributions from the linkage preferential binding increments for protons and magnesium ions, which are ca. −1 and 1, respectively.

The difference of the van't Hoff enthalpy from the calorimetric enthalpy change of taxol-induced assembly in PEDTA and 4 mM $MgCl_2$ buffer, pH 6.7, is 164 kJ mol^{-1} (Tables I and II). As has been discussed (Lee & Timasheff, 1977; Hinz et al., 1979), the van't Hoff enthalpy is a complex summation of all the individual heats through a proper combination of equilibrium constants and activities of reactants. In our case this simplifies to the apparent enthalpy change of the growth reaction, which includes a contribution due to the linked binding of two Mg^{2+} ions. In calorimetric measurements the apparent enthalpy value is the algebraic sum of all the heat processes, which would include in principle nucleation, addition of the molecule of tubulin to the growing polymer, taxol binding, and the binding of Mg^{2+} ions. The variations found in the observed enthalpy of assembly and in the curve shape at high Mg^{2+} concentrations could suggest that an important part of the heat absorption associated with the process would have taken place at the initial temperature of the DSC experiment. Neglecting the contributions due to the association of the small percent of protein molecules which should participate in the nucleation reaction (Hinz et al., 1979), and according to Scheme I, under excess ligand concentration tubulin could probably be bound to the ligand at the beginning of the DSC scan, and therefore the calorimetric minus the van't Hoff enthalpy would correspond to a function of the enthalpy change of Mg^{2+} binding and the cation concentration, plus the contribution of any other processes whose degree of completion could be strongly affected by the temperature within the interval between the two measurements. According to Scheme II, there should not be any ligand binding when the DSC experiment is started, since there are no preformed microtubules, and therefore the calorimetric minus the van't Hoff enthalpy should include in addition the enthalpy of binding of the ligand to the microtubule end.

Examination of the extents of binding and polymerization as functions of the ligand concentration (Figure 7) confirmed that the two processes are tightly coupled under present experimental conditions. Both show a cooperative behavior which made linear Wyman plots of the data according to eq 3 (Materials and Methods) not applicable. Similarly, numerical simulations employing simple models, such as Schemes I and II (eqs 7 and 18), were inaccurate. This is because at nonsaturating ligand concentrations, under the conditions of Figure 7, the concentration of unassembled protein depends on the total protein concentration, and sharp critical protein and ligand concentrations do not exist. This does not affect the rest of the study, in which the measurements of K_{app} were made at saturating ligand concentrations. Out of the narrow assembly conditions (protein and Mg^{2+} concentration) of Figure 7, the bulk of ligand added below the total protein concentration was bound by the induced polymer and the very small free ligand concentration left could not be measured accurately. Detailed examination of the system in terms of the ligand-linked aggregation and phase equilibria theories, which have been applied to hemoglobin (Wyman & Gill, 1980; Gill et al., 1980; Wyman & Gill, 1990), appears to be precluded due to the fact that reactions 4 and 3 (Scheme I) could not be characterized for GDP–tubulin under present conditions, but this might be feasible by employing nonhydrolyzable GTP analogues.

Model Mechanisms of Taxol- and Taxotere-Induced Assembly. GDP–tubulin is totally unable to assemble spontaneously and form microtubules under normal conditions and has been regarded as having a curved conformation which favors the formation of double rings (Howard & Timasheff, 1986; Melki et al., 1989; Shearwin & Timasheff, 1992). It has been reported that GDP–tubulin binds nonproductively to microtubule ends, with an equilibrium association constant 3–5 times smaller than that of GTP–tubulin (i.e., a difference free energy change of only 3.5 ± 0.7 kJ mol^{-1}), and blocks elongation (Carlier et al., 1987). Direct photoaffinity labeling of microtubules with taxol has indicated that this ligand binds to β-tubulin (Rao et al., 1992) as the exchangeable nucleotide (Farr & Sternlicht, 1992). Back-substitution of the nucleotide γ-phosphate in the taxoid-induced microtubule assembly system results in an effective increment elongation free energy change value of $\Delta\Delta G^\circ_{app}$(GTP–GDP) = $\Delta\Delta G^\circ_2$(GTP–GDP) = −2.5 ± 0.4 kJ mol^{-1} under a variety of experimental conditions (Table I; Díaz & Andreu, 1993). This effect of the γ-phosphate could possibly be more rigorously measured by employing nonhydrolyzable GTP analogues. We wish to propose the hypothesis that taxoid binding favors the straight microtubule forming protein conformation, rendering the association of GDP–tubulin productive for elongation. The taxoid induction of microtubule elongation may be envisaged to proceed by means of allosteric or contact mechanisms as exemplified for the purpose of this discussion by the schemes of Figure 9 (models A and B, respectively). In these models the ratio of the apparent elongation equilibrium constants of the GTP– and GDP–tubulin forms is just a reflection of their relative affinity for the microtubule end in the absence of drug. In the former type of models the binding of the ligand induces a straight protein conformation (either in unassembled tubulin, AI, or in tubulin at the microtubule end, AII) which is able to associate better to other protein molecule(s). While the exclusively allosteric A models would proceed by a presently

[3] The thermodynamic cycle of Scheme I may also be considered in the presence of glycerol. In 3.4 M glycerol-containing buffer, ΔG°_4 = −28 ± 0.6 kJ mol^{-1} (Table I). The critical concentration for assembly with ligand plus glycerol has been measured, and the resulting standard free energy change values are −34.6 ± 0.7 (taxol) and 36.3 ± 0.6 kJ mol^{-1} (Taxotere) under identical conditions. Therefore, in glycerol buffer the values of $\Delta G^\circ_{linkage}$ would be −6.6 ± 0.7 and −8.3 ± 0.6 kJ mol^{-1}, respectively, which is ca. 4 kJ mol^{-1} more positive than in the absence of glycerol and could indicate an effect of this cosolvent on the system.

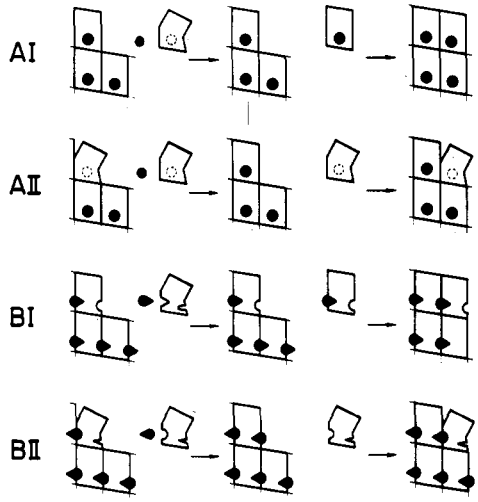

FIGURE 9: Possible model mechanisms of taxoid-induced elongation of GDP–tubulin. The ligand-mediated addition of one tubulin molecule to the microtubule lattice is represented. The unliganded protein is in the curved conformation, which polymerizes in ring fashion but blocks further elongation at the microtubule end. Taxoid binding favors the straight tubulin conformation, which elongates microtubules. The linkage of the binding of the taxoid (solid circles) to the tubulin–tubulin contact formation either is purely allosteric (models AI and AII), or also involves the participation of the ligand (solid circular sectors) in the protein-binding interface (models BI and BII). It is assumed that the ligand binds either to unassembled tubulin (I models) or to tubulin at the microtubule end (II models). Model AII is the same as the ligand-facilitated pathway corresponding to the ligand-mediated model AI. Since the available data support the participation of a ligand-mediated pathway, model AII might be discarded. On the contrary, given the fact that binding of taxoid to the unassembled tubulin has not been observed, the II models might be favored over the I models. Therefore, it would appear that the A models are contradictory. However, if taxoid binding would induce another conformation in the structure of unassembled tubulin by preferential binding to a new conformation not significantly populated in the absence of ligand, and this conformation had a large affinity for the microtubule end, the polymer would exist in equilibrium with unliganded protomer, and liganded unassembled protein would not be observed. Note that in the particular II models employed the binding to tubulin at the microtubule end is linked to an increase in the contact area with the underlying tubulin molecule and is of greater affinity than the equivalent binding to unassembled tubulin. Alternatively, II′ models may be considered in which tubulin remains in the curved conformation after taxol binding, and it is the addition of the next protomer that leads to the straight conformation. Model BII′ would be a purely contact model; however, the binding of the ligand to the high-affinity half-site would be expected to have the same affinity in soluble tubulin as in the microtubule.

unknown conformational mechanism, in the B models the taxoid is a double-sided ligand which first binds to the protein (either tubulin BI, or the microtubule end, BII) and forms part of one of the protein–protein association interfaces. In the contact-allosteric schemes (B models) the taxoid would fill an accessible cavity, contributing to the contacts between tubulin subunits. The marked changes observed in the thermodynamic parameters of the elongation reaction strongly suggest changes in the nature of contacts between tubulin molecules. The contact models also appear attractive because they are simple and are supported by the X-ray scattering analysis of the low-resolution structure of microtubules in solution, which has shown taxoid-induced changes in the lateral contact angle between protofilaments (Andreu et al., 1992; Peyrot et al., 1992); they are compatible with the proposal that the taxol side chain binds to a crevice in the protein (Swindell et al., 1991) and with the suggestion that taxol induces the lateral association of tubulin molecules in the microtubule wall (Howard & Timasheff, 1988). In model BII the linkage free energy provided by the ligand binding is

Scheme III

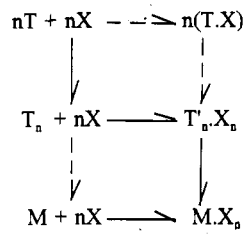

the unitary free energy change of binding of the taxoid to the second half-site on the adding tubulin molecule (which, given the protein association, is a unimolecular ligand to protein binding reaction). Its value, ca. −10 kJ mol^{-1}, corresponds to a weak interaction. Such interaction would only be effective in the species MXT, since the interaction of the ligand with unassembled tubulin to form the species XT would be characterized by a nil observed free energy change, which results from the addition of the unitary free energy change and the ca. 10.3 kJ mol^{-1} cratic free change term arising from the change of entropy of mixing in the system in the bimolecular binding reaction (Andreu & Timasheff, 1982). If model BI was correct, instead of model BII, the high- and low-affinity half-sites would just be reversed. In these contact models taxol is a molecular matchmaker (Ringe, 1992), which creates a new surface and facilitates the macromolecular recognition between protein subunits, similarly to cyclosporin A in the decameric cyclophilin complex structure and possibly also in the interaction with calcineurin (Pflügl et al., 1993).

Schemes I and II have been proposed to analyze the thermodynamics of the taxol-induced microtubule elongation. However, the species M in these schemes stands for the unliganded microtubule ends, and it is implicitly assumed that the body of such microtubules contains one ligand bound per tubulin dimer, since they come from previous elongation steps. The question is how the first liganded microtubules are formed, that is, which is the kinetic mechanism of nucleation. The GTP–tubulin concentrations employed are at least 1 order of magnitude smaller than the critical protein concentration required for ligand-independent microtubule assembly under the conditions employed. Therefore, spontaneously formed microtubules would exist only in vanishingly small concentration in the solution. If they were the polymerization nuclei, the ligand-induced assembly would be expected to be extremely slow. This is contrary to observation, since taxol microtubules polymerize with characteristically smaller lag time and critical concentration than drug-free ones. This is particularly obvious for GDP–tubulin, which has not been observed to assemble into microtubules, except with the taxoids. The conclusion follows that these ligands should induce nucleation by binding to intermediate species in the assembly pathway, i.e., to tubulin oligomers. This is exemplified in Scheme III. In this model the hypothesis is made that the binding of taxol to the preexisting assembly-inactive oligomer, T_n, transforms it into the actively assembling nucleating species $T'_n{\cdot}X_n$. According to this scheme, purified calf brain tubulin without Mg^{2+}, which is in the dimer form even at unusually high protein concentrations (Andreu et al., 1989), does not undergo assembly because it does not form oligomers. On the other hand, Mg^{2+} is known to induce the isodesmic self-association of purified tubulin, leading to double ring formation (Frigon & Timasheff, 1975a,b; Howard & Timasheff, 1986). Under appropriate conditions microtubules are formed instead of rings (Lee & Timasheff, 1975, 1977). Taxol binding, under conditions of incipient tubulin self-association induced by Mg^{2+}, promotes the assembly of microtubules, in support of Scheme III. This

type of mechanism could also explain the marked protein concentration dependence of the polymerization observed at nonsaturating ligand concentrations (Figure 7). Similarly to elongation, taxol could induce the lateral accretion of tubulin molecules of small linear oligomers to form bidimensional polymerization nuclei.

ACKNOWLEDGMENT

We thank Dr. V. Peyrot and Dr. C. Briand, Faculté de Pharmacie de Marseille, for extensive discussion and support, Dr. G. Rivas and one anonymous reviewer for helpful suggestions, Dr. J. L. Fabre, Rhône-Poulenc Rorer (Antony, France), for Taxotere and ^{14}C-Taxotere, Dr. M. Suffness, National Cancer Institute (Bethesda, MD), for taxol, Dr. I. Ringel, Hebrew University (Jerusalem) and Dr. S. B. Horwitz, Albert Einstein College of Medicine (Bronx, NY), for ^{3}H-taxol. We wish to acknowledge the help of A. Hurtado with the drawings.

REFERENCES

Andreu, J. M., & Timasheff, S. N. (1982) *Biochemistry 21*, 534–543.
Andreu, J. M., Wagenknecht, T., & Timasheff, S. N. (1983) *Biochemistry 22*, 1556–1566.
Andreu, J. M., García de Ancos, J., Starling, D., Hodgkinson, J. L., & Bordas, J. (1989) *Biochemistry 28*, 4036–4040.
Andreu, J. M., García de Ancos, J., Medrano, F. J., Gil, R., Díaz, J. F., Nogales, E., Towns-Andrews, E., Pantos, E., & Bordas, J. (1991) *AIP Conf. Proc. No. 227*, 160–169.
Andreu, J. M., Bordas, J., Díaz, J. F., García de Ancos, J., Gil, R., Medrano, F. J., Nogales, E., Pantos, E., & Towns-Andrews, E. (1992) *J. Mol. Biol. 226*, 169–184.
Arriaga, P., Menendez, M., Martin Villacorta, J., & Laynez, J. (1992) *Biochemistry 31*, 6603–6607.
Aune, K. C., Goldsmith, L. C., & Timasheff, S. N. (1971) *Biochemistry 10*, 1617–1622.
Cantor, C. R., & Schimmel, P. R. (1980) *Biophysical Chemistry*, Freeman, San Francisco.
Carlier, M. F., & Pantaloni, D. (1983) *Biochemistry 22*, 4814–4822.
Carlier, M. F., Didry, D., & Pantaloni, D. (1987) *Biochemistry 26*, 4428–4437.
Collins, C. A., & Vallee, R. B. (1987) *J. Cell Biol. 105*(6) 2847–2854.
Díaz, J. F., & Andreu, J. M. (1993) *Biochemistry 32*, 2747–2755.
Erickson, H. P. (1989) *J. Mol. Biol. 206*, 465–474.
Erickson, H. P., & Pantaloni, D. (1981) *Biophys. J. 34*, 293–309.
Farr, G. W., & Sternlicht, H. (1992) *J. Mol. Biol. 227*, 307–321.
Foster, K. E., & Rosemeyer, M. A. (1986) *FEBS Lett. 194*, 78–84.
Frigon, R. P., & Timasheff, S. N. (1975a) *Biochemistry 14*, 4559–4566.
Frigon, R. P., & Timasheff, S. N. (1975b) *Biochemistry 14*, 4567–4573.
Gaskin, F., & Kress, Y. (1977) *J. Biol. Chem. 252*, 6918–6924.
Gaskin, F., Cantor, C. R., & Shelanski, M. L. (1974) *J. Mol. Biol. 89*, 737–758.
Gill, S. J., Spokane, R., Benedict, R. C., Fall, L., & Wyman, J. (1980) *J. Mol. Biol. 140*, 299–312.
Himes, R. H., Burton, P. R., & Gaito, J. M. (1977) *J. Biol. Chem. 252*, 6222–6228.
Hinz, H. J., & Timasheff, S. N. (1986) *Biochemistry 25*, 8285–8291.
Hinz, H.-J., Gorbunoff, M. J., Price, B., & Timasheff, S. N. (1979) *Biochemistry 18*, 3084–3089.
Horwitz, S. B. (1992) *Trends Pharmacol. Sci. 13*, 134–136.
Howard, W. D., & Timasheff, S. N. (1986) *Biochemistry 25*, 8292–8300.
Howard, W. D., & Timasheff, S. N. (1988) *J. Biol. Chem. 263*, 1342–1346.
Lee, J. C., & Timasheff, S. N. (1975) *Biochemistry 14*, 5183–5187.
Lee, J. C., & Timasheff, S. N. (1977) *Biochemistry 16*, 1754–1764.
Medrano, F. J., Andreu, J. M., Gorbunoff, M. J., & Timasheff, S. N. (1991) *Biochemistry 30*, 3770–3777.
Mozo-Villarías, A., Morros, A., & Andreu, J. M. (1991) *Eur. Biophys. J. 19*, 295–300.
Na, G. C., & Timasheff, S. N. (1980) *Biochemistry 19*, 1355–1365.
Na, G. C., & Timasheff, S. N. (1981) *J. Mol. Biol. 151*, 165–178.
Oosawa, F., & Asakura, S. (1975) *Thermodynamics of the Polymerization of Protein*, Academic Press, London.
Parness, J., & Horwitz, S. B. (1981) *J. Cell Biol. 91*, 479–487.
Peyrot, V., Briand, C., Díaz, J. F., & Andreu, J. M. (1992) Meeting on Drugs and Microtubules, Marseille, France, *Maimonide 1*, S22.
Pflügl, G., Kallen, J., Schrimer, T., Jansonius, J. N., Zurini, M. G. M., & Walkinshaw, M. D. (1993) *Nature 361*, 91–94.
Rao, S., Horwitz, S. B., & Ringel, I. (1992) *J. Natl. Cancer Inst. 84*, 785–788.
Ringe, D. (1992) *Curr. Biol. 2*, 545–551.
Ringel, I., & Horwitz, S. B. (1991) *J. Pharmacol. Exp. Ther. 259* (2), 855–860.
Sanchez-Ruiz, J. M., Lopez-Lacomba, J. L., Cortijo, M., & Mateo, P. L. (1988) *Biochemistry 27*, 1648–1652.
Swindell, C. S., Krauss, N. E., Horwitz, S. B., & Ringel, I. (1991) *J. Med. Chem. 34*, 1176–1184.
Takoudju, M., Wright, M., Chenu, J., Guéritte-Voelgelein, F., & Guénard, D. (1988) *FEBS Lett. 227*, 96–98.
Tanford, C. (1969) *J. Mol. Biol. 39*, 539–544.
Timasheff, S. N. (1981) in *Protein–Protein Interactions* (Frieden, C., & Nichol, L. W., Eds.) pp 315–336, Wiley, New York.
Wilson, L., Miller, H. P., Farrell, K. W., Snyder, K. B., Thompson, W. C., & Purich, D. L. (1985) *Biochemistry 24*, 5254–5262.
Wyman, J. (1964) *Adv. Protein Chem. 19*, 224–285.
Wyman, J., & Gill, S. J. (1980) *Proc. Natl. Acad. Sci. U.S.A. 77*, 5239–5242.
Wyman, J., & Gill, S. J. (1990) *Binding and linkage*, University Science Books, Mill Valley, CA.